# Desulfurization of Model Oil *via* Adsorption by Copper(II) Modified Bentonite

**Dezhi Yi, Huan Huang, and Li Shi[*]**

*The State Key Laboratory of Chemical Engineering, East China University of Science and Technology, Shanghai 200237, China*
*[*]E-mail: yyshi@ecust.edu.cn*

In order to further reduce the sulfur content in liquid hydrocarbon fuels, a desulfurization process by adsorption for removing dimethyl sulfide (DMS) and propylmercaptan (PM) was investigated. Bentonite adsorbents modified by $CuCl_2$ for the desulfurization of model oil was investigated. The results indicated that the modified bentonite adsorbents were effective for adsorption of DMS and PM. The bentonite adsorbents were characterized by X-ray diffraction (XRD) and thermal analysis (TGA). The acidity was measured by FT-IR spectroscopy. Several factors that influence the desulfurization capability, including loading and calcination temperature, were studied. The maximum sulfur adsorption capacity was obtained at a Cu(II) loading of 15 wt %, and the optimum calcination temperature was 150 $^{\circ}$C. Spectral shifts of the $\nu$(C-S) and $\nu$(Cu-S) vibrations of the complex compound obtained by the reaction of $CuCl_2$ and DMS were measured with the Raman spectrum. On the basis of complex adsorption reaction and hybrid orbital theory, the adsorption on modified bentonite occurred *via* multilayer intermolecular forces and S-M ($\sigma$) bonds.

**Key Words :** Dimethyl sulfide, Propylmercaptan, Bentonite, Adsorption, Mechanism

## Introduction

The requirement of ultraclean transportation fuels, particularly, gasoline, diesel, and jet fuels, has resulted in a continuing worldwide effort to dramatically reduce the sulfur levels in them.[1] The presence of sulfur compounds in these fuels are the main cause of acid rain and poisoning of catalysts in CO and $NO_x$ catalytic converters. The issues of gasoline and diesel deep desulfurization are becoming more serious because crude oils refined in various countries are becoming higher in sulfur content and heavier in density, while the regulated sulfur limits are becoming lower and lower. Strict environmental regulations require the removal of sulfur from gasoline to very low (< 20 ppm) levels.[2] Therefore, they are facing the challenge of producing increasingly cleaner fuels. In conventional removal of sulfur compounds, hydrodesulfurization (HDS) processes are carried out, using Co-Mo/$Al_2O_3$ or Ni-Mo/$Al_2O_3$ catalysts at high temperatures (300-340 $^{\circ}$C) and pressures (20-100 atm of $H_2$) conditions.[3] However, HDS processes cannot meet the current sulfur level requirements, and the hydrogenation of olefins should be simultaneously minimized, because it reduces the octane number.

Thioether and thiol, with strong odors, are contained in crude oil and their products and volatile compounds will be emitted into the atmosphere. Therefore, to reduce the sulfur that is involved in the storage, transportation, and refining process of oils has become an important worldwide issue to refinery engineers.[4,5] In this case, adsorptive desulfurization, which could be accomplished at ambient temperature and pressure, is considered to be a promising approach. Deep desulfurization on various adsorbents such as activated carbons (ACs),[6-9] modified composite oxide,[10] and zeolite,[11-13]

has already been studied. Because of its physical and chemical properties (*i.e.*, large specific surface area and adsorptive affinity for organic and inorganic ions), bentonite is increasingly attracted widespread attention as a new type of microporous solid that can serve as separating agents or sorbents, *etc.*

In this paper, the main objective of the present study is to investigate the efficiency of modified bentonite for the removal of dimethyl sulfide (DMS) and propylmercaptan (PM). The bentonite adsorbents was characterized by X-ray diffraction (XRD), thermal analysis (TGA) and FT-IR spectroscopy. The Cu(II) complexe was characterized by the Raman spectrum. And the adsorption mechanism was explained in combination with the hybrid orbital theory.

## Experimental Section

**Materials.** In this study, the raw activated bentonite was obtained from Zhejiang Province, China. The composition analysis (mass %) is shown in Table 1. $CuCl_2$ were purchased

**Table 1.** The composition of Lin An activated bentonite

| Components | wt % |
|---|---|
| $SiO_2$ | 67.8 |
| $Al_2O_3$ | 16.3 |
| $Fe_2O_3$ | 4.0 |
| MgO | 0.4 |
| CaO | 1.1 |
| MgO | 1.7 |
| $K_2O$ | 1.6 |
| $Na_2O$ | 0.9 |
| Others | 7.0 |

from Sinopharm Chemical Reagent Co., Ltd. DMS and PM were purchased from Shanghai Chemical Reagent Co., Ltd. The sorbents used were prepared *via* a kneading method, using raw activated bentonite and $CuCl_2$. Raw activated bentonite and $CuCl_2$ with different content were sufficiently mixed for 0.5 h. Then, a liquid binder, dilute nitric acid, was added to the mixture to make the slurry. An extruder was used to formulate pellets to an outer diameter of 1 mm from the slurry. All of the sorbents were dried at 120 ℃ for 2 h, baked in a muffle furnace in $N_2$ for 2 h, and crushed and screened to 20-40 mesh before use.

To obtain the model oil for desulfurization, DMS and PM were simultaneously placed into *n*-hexane and the sulfur content of model oil of DMS and PM was 2000 ppm, respectively.

**Sulfur Adsorption Experiments.**

**Dynamic Tests:** Dynamic tests were carried out to evaluate the capacity of the sorbents for sulfur removal. First, adsorbent samples were packed into a quartz column (length: 500 mm; internal diameter: 9 mm; bed volume: 1.25 cm$^3$). Then the sorbent was loaded in the middle of the reactor and the spare spaces were filled with quartz sand (20-40 mesh). The experiments were carried out under the following conditions: atmospheric pressure, LHSV (liquid hourly space velocity) 5.0 h$^{-1}$. The outflow oil was analyzed with a Hewlett-Packard HP5890 gas chromatograph equipped with flame ionization detection (FID) and gas chromatography-mass spectroscopy (GC-MS) (Agilent GC 6890-MS 5973 N):

$$\text{Desulfurization ration (\%)} = [(C_0 - C)/C_0] \times 100$$

$$\text{Sulfur capacity (mg-S/g of adsorbent)} = \frac{(C_0 - C)VM}{m} \times 1000$$

Where $C_0$ is the initial number of moles of sulfur (mol/L), $C$ is the final number of moles of sulfur (mol/L), $V$ is the volume of solution (L), $M$ is the molar mass of sulfur (g/mol), and m is the weight of sorbent (g).

**Static Tests:** Static tests were carried out at ambient temperature to evaluate the capacity of the sorbents for sulfur removal. Adsorbent (0.2 g) was added to a 20 mL sample of hydrocarbon containing sulfur in an airtight container with a shaker apparatus operating at ambient temperature for 2 days. Then the concentration of sulfur was analyzed by gas chromatography.

**Preparation of the Cu(II) Complexe:** The Cu(II) complexe were prepared by mixing an excess of DMS with $CuCl_2$ in an airtight container through the static complex adsorption for 2 days. The deposit formed during the reaction was vacuum filtered and subsequently extensively washed with n-hexane. The products were left to dry at room temperature.

**Analysis.**

**X-ray Diffraction:** X-ray diffraction (XRD) technique was used to characterize the crystal structure. In this work, XRD patterns were obtained with a Siemens Model D-500 X-ray diffractometer equipped with Ni-filtered Cu KR radiation (40 kV, 100 mA). The 2θ scanning angle range was 10-80° 

with a step of 0.02(°)/s.

**The Molar Ratio of Copper and Sulfur:** In order to verify the complex compound, concentration of copper and sulfur of the deposit were measured. ICP-ICP-AES measurements, for the determination of total copper in solid sample, were made in the inductively coupled plasma-atomic emission spectrometer (ICP-AES) Varian 700. The sulfur analysis was performed by the Antek 9000S/N.

**FT-IR Spectroscopy:** The amount of acid, acid density, and acid variety were measured *via* Fourier transform infrared (FT-IR) spectroscopy (Nicolet Company, Model Magna-IR550), using pyridine as the probe molecule. There are two varieties of acid: one is a Brønsted acid (denoted as B), whose characteristic absorption peak is observed at 1540 cm$^{-1}$; and the other is a Lewis acid (denoted as L), whose characteristic absorption peak is located at 1450 cm$^{-1}$. The pyridine adsorption, which is measured after desorption at 200 ℃, is the total acid sites (T). The pyridine adsorption, which is measured after desorption at 450 , represents the strong acid sites (S). The difference represents the weak acid sites (W).

**Thermal Analysis:** Thermo-gravimetric (TG) curves were obtained using a TA Instruments thermal analyzer. The samples were exposed to an increase in temperature of 10 ℃/min up to 700 ℃ while the nitrogen flow rate was held constant at 100 mL/min.

**Raman Spectra:** The Raman spectra studies were conducted on a Renishaw System 100 Raman spectrometer using 514 nm red excitation from an Ar laser. The laser power was 3 mW at the sample position. The Raman scattered light was detected perpendicular to the laser beam with a Peltier-cooled CCD detector, and the spectral resolution in all measurements was 1 cm$^{-1}$.

## Results and Discussion

**XRD Characterizations of the Modified Bentonite Adsorbents.** X-ray diffraction analysis in Figure 1 was carried
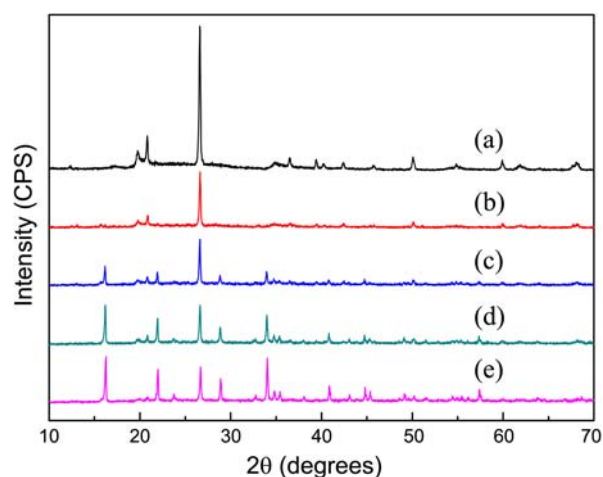


**Figure 1.** X-ray diffraction patterns of Cu(II)-bentonite calcinated at 150 ℃ with different Cu(II) content: (a) raw bentonite, (b) 5 wt %, (c) 10 wt %, (d) 15 wt % and (e) 20 wt %.
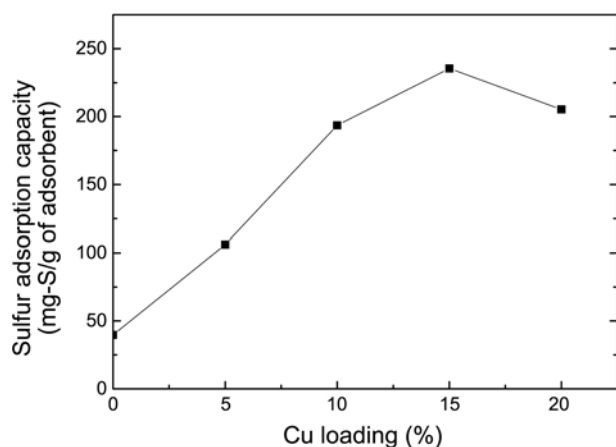
**Figure 2.** Sulfur adsorption capacity with different amounts of Cu(II) loading on bentonite at calcination temperature of 150 ℃.

out to identify the mineralogical structure of the modified bentonite adsorbents. The existence of diffraction reflections in the angle region indicates that our samples had ordered structure on the micropore scale. The XRD patterns of the bentonite adsorbents loaded with CuCl₂ showed the characteristic reflections for CuCl₂ at 2θ = 16.19°, 21.93° and 33.96° corresponding to the planes (110), (020) and (201) of cubic CuCl₂ crystal, respectively.[14] Figure 1 confirmed that the concentration of CuCl₂ increased with an increasing Cu(II) content, and the crystallinity of the modified bentonite adsorbents slightly decreased, compared to raw bentonite, because of the framework defects caused by the loading metal ion. These facts suggested that CuCl₂ on the bentonite existed as amorphous materials with a low Cu(II) content. And with the increasing of Cu(II) content, CuCl₂ on the bentonite existed as crystalline solid. Excessive CuCl₂ would block the pores of the bentonite adsorbents, and the adsorption rate would decrease.

**Effects of the Amount of Cu Loading on Adsorption of DMS and PM.** Dynamic tests and static tests were carried out at room temperature to evaluate the capacity of the sorbents for sulfur removal. A correlation between desulfuration and different concentration of Cu loadings of activated bentonite has been tested; the static test results shown in Figure 2 and the dynamic test results presented in Figure 3 denoting the breakthrough curves for DMS and PM.

It can be seen from the curves shown in Figure 2 and Figure 3 that the bentonite loaded with CuCl₂ could absorb more sulfur than the raw bentonite. In accordance with the static tests, the sulfur capacity of dynamic tests was increased gradually with an increasing amount of Cu(II) loading. When the amount of Cu(II) loading was 15 wt %, the sulfur adsorption capacity reached a maximum, was 235 mg-S/g of adsorbent.

The results showed that bentonite loaded with CuCl₂ could be proper adsorbents for the removal of sulfur from model oil. Thiols are active organic sulfide and thiolate conjugate bases are easily formed. It is reported that copper(II) reacted with thiol and formed copper(II) mercaptide.[15] As is shown in listed reactions (1), thiolate copper(II) mercaptide could
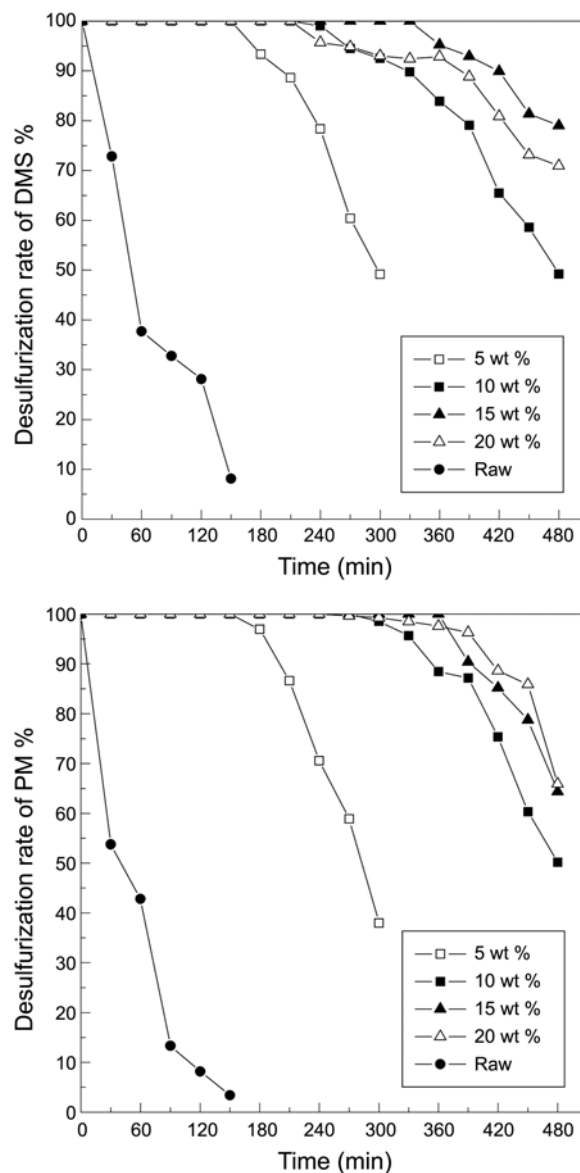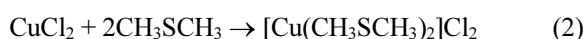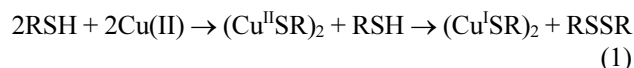




**Figure 3.** Breakthrough curves for DMS and PM adsorption on different Cu(II) loadings of bentonites at calcination temperature of 150 ℃.

obtained by the reaction of Cu(II) and thiols. It can be seen that $(Cu^{II}SR)_2$ in excess of thiol could be decomposed leading to copper(I), thiol radical, and forming $(RSCu^I)_2$ and disulfide.

$$2RSH + 2Cu(II) \rightarrow (Cu^{II}SR)_2 + RSH \rightarrow (Cu^ISR)_2 + RSSR \tag{1}$$

$$CuCl_2 + 2CH_3SCH_3 \rightarrow [Cu(CH_3SCH_3)_2]Cl_2 \tag{2}$$

As is shown in listed reactions (2), the complex compound which was a brown deposit was obtained though the complex adsorption of CuCl₂ and DMS. In order to verify the complex compound, concentration of copper and sulfur of the deposit were measured by inductively coupled plasma-atomic emission spectroscopy (ICP-AES) and Antek 9000S/N. The Cu content of the deposit was 25.6 wt % and sulfur
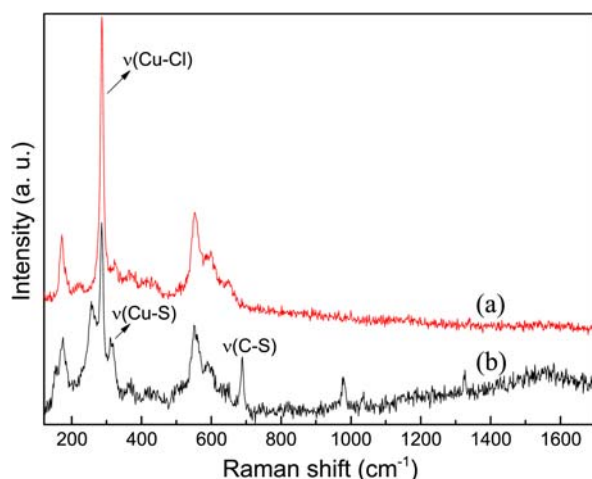
**Figure 4.** The Raman spectrum of CuCl₂ and the complex compound: (a) CuCl₂, (b) complex compound.

content was 24.7 wt %. The molar ratio S/Cu = 2 was obtained. The electronegativity of sulfur atom is not so high and it is easy to lose the lone electron pairs. Atoms of $Cu^{II}(1s^2 2s^2 2p^6 3s^2 3p^6 3d^9 4s^0)$ can form the usual σ bonds with their empty *s*-orbitals, and *p*-orbitals. Mixing one s orbital and three p orbitals gives four sp³ hybrid orbitals, which are directed toward a tetrahedral structure. The sulfur atoms of DMS provide lone pair electrons to Cu(II) and form the usual S-M (σ) bonds.[16,17]

Figure 4 presents the Raman spectrum of CuCl₂ and the complex compound obtained by the reaction of CuCl₂ and DMS. The features at 305 cm⁻¹ are not observed in the spectrum of CuCl₂, but are seen in the spectrum of the Cu(II) complexe.[18] This region is characteristic of the Cu-S stretching vibrations, suggesting that DMS should bind to the Cu(II) with its sulfur atom. The curve B presents bands at 690 cm⁻¹, arising from ν(C-S) vibration of DMS adsorbed at Cu(II).[19] This result suggests that DMS may adsorb on CuCl₂ without cleavage of its C-S bond.

**FT-IR Spectra of the Bentonite Adsorbents.** In order to investigate the type and number of surface acidic sites on the bentonite adsorbents, FT-IR spectra for the adsorption of pyridine at 200 and 450 were obtained as shown in Figure 5. The spectrum displayed many bands in the wavenumber range of 1400-1600 cm⁻¹, which was attributed to the interaction of pyridine with Lewis (L) and Brønsted (B) acid sites on the sample surfaces. As shown in Figure 5, the spectra presented bands of adsorption at 1450 cm⁻¹, arising from ν(C-C) vibration of pyridine adsorbed at Lewis acid sites.[20] From Figure 5, we can see that the peak of curve a at 1450 cm⁻¹ was higher than that of curve b. This indicated that the total number of Lewis acid sites on the surface of bentonite loaded with CuCl₂ was stronger than that of raw bentonite, and the Lewis acid sites would be increased after metals insertion. And in comparison to the adsorption of pyridine at 200 ºC, the peak of curve a at 1450 cm⁻¹ at 450 ºC was weaker. It was showed that high calcination temperature could reduce the total number of Lewis acid sites.

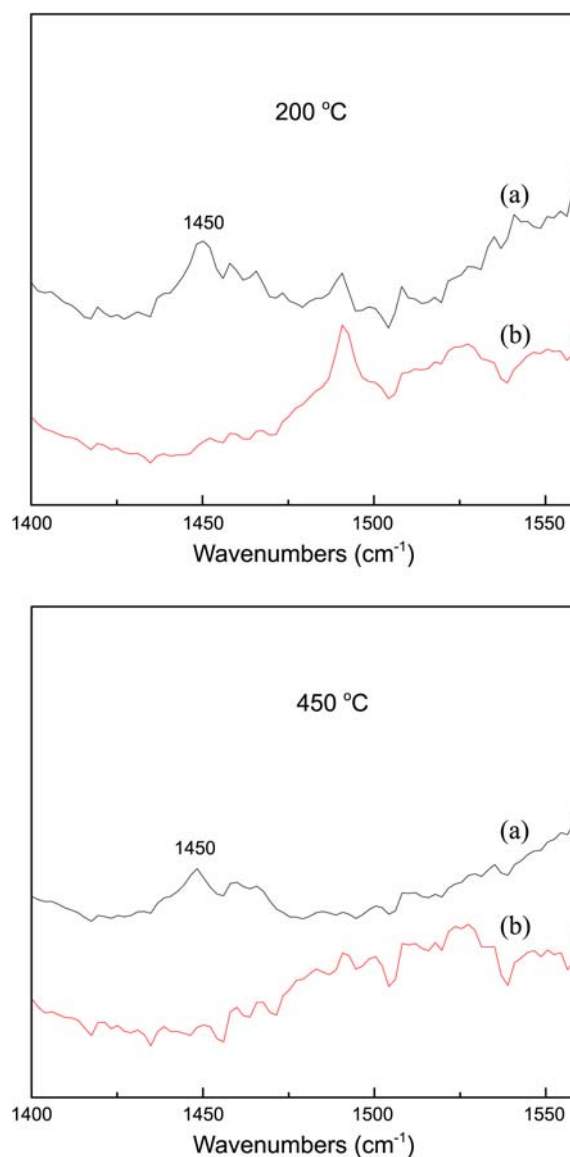**Effects of Baking Temperature on the Adsorption of**



**Figure 5.** FT-IR spectra of two adsorbents at 200 ºC and 450 ºC: Cu(II)-bentonite (spectrum a) and raw bentonite (spectrum b).

**Sulfur.** Different baking temperatures ranging from 120 ºC to 450 ºC were tested on 15 wt % Cu(II)-bentonite. Under the different calcination temperatures, the static desulfurization effects of the absorbents were collected, as shown in Figure 6. It reveals that the optimal calcination temperature of the modified bentonite adsorbents was 150 ºC. As the calcination temperature increased from 150 ºC to 450 ºC, the sulfur removal ability of the adsorbents was gradually reduced. Compounds on the surface of bentonite at a calcination temperature of 150 ºC may be present mostly in the form of CuCl₂. The influence of calcination temperature was evaluated using the TA method combined with XRD. The differential scanning calorimetry-thermogravimetric analysis (DSC-TGA) curves for our adsorbents were collected and are shown in Figure 7. A considerable weight loss was observed for the raw and modified bentonite. From the DTG curves of bentonite loaded with CuCl₂, the two peaks in the
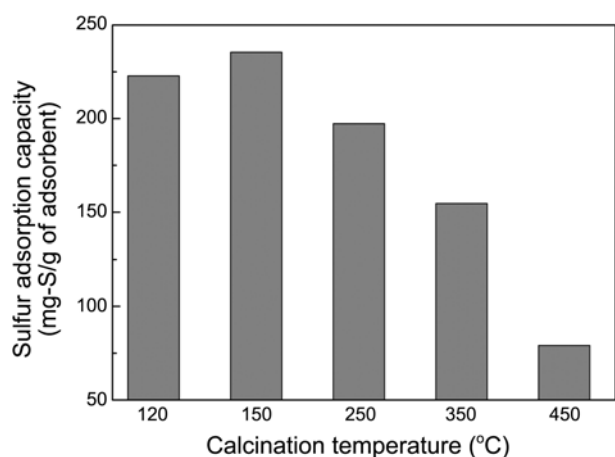
**Figure 6.** Effect of baking temperature on adsorption capacity of 15 wt % Cu(II)-bentonite.
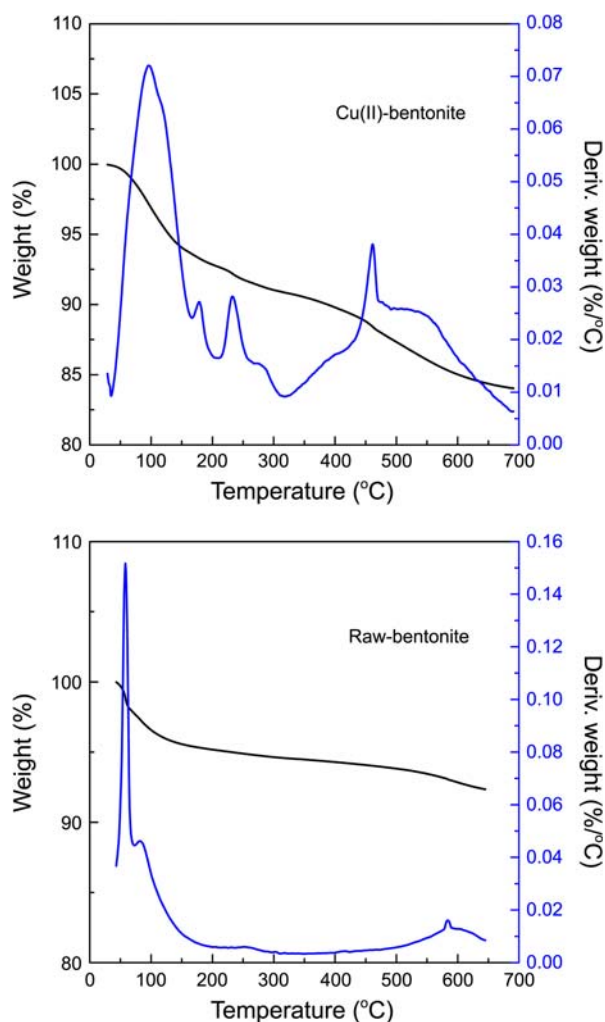


**Figure 8.** X-ray diffraction patterns on 15 wt % Cu(II)-bentonite with different calcination temperatures: (a) 150 $^{\circ}$C, (b) 250 $^{\circ}$C, (c) 350 $^{\circ}$C and (d) 450 $^{\circ}$C.

not only the further oxidation of Cu but also by the volatilization of compounds. In curve of raw bentonite, no peak was found between 200-500 $^{\circ}$C, this indicated that the framework of bentonite is stable below 500 $^{\circ}$C. It indicated that, because of the capillary force of adsorbent's micropore, when the calcination temperature was 120 $^{\circ}$C, some water was absorbed in the adsorbents and some crystal water did not evaporate and would block the pores of the adsorbents.

The modified bentonite baked at different calcination temperature were further characterized by X-ray diffraction (XRD) to get more structural information, as shown in Figure 8. The sample calcined at 150 $^{\circ}$C showed the presence of the $CuCl_2$ phase and the intense peaks of $CuCl_2$ decreased with increasing calcination temperature in 15% Cu(II)-bentonite sorbent systems. When the sample calcined at 250 $^{\circ}$C and 350 $^{\circ}$C, XRD reflections due to crystalline CuCl are noticed at $2\theta = 15.95°$ and $32.41°$, and the intensities of these reflections are found to increase with the increase of calcination temperature. At higher calcination temperature (from 400 $^{\circ}$C), the XRD patterns of the modified bentonite adsorbents showed the characteristic reflections for CuO at $2\theta = 35.54°$ and $38.71°$, suggesting that CuCl decompose to CuO. Combined with XRD, the results from the DSC-TGA curves of modified bentonite correspond to extensive weight loss *via* the stepwise decomposition of $CuCl_2·2H_2O$: [21]

$$CuCl_2·2H_2O \rightarrow CuCl_2 \rightarrow CuCl \rightarrow CuO$$

From the results obtained by XRD and the DSC-TGA curves, it is inferred that modifier on the surface of bentonite with a calcination temperature of 150 $^{\circ}$C may be present, mostly in their own form $CuCl_2$. However, as the calcination temperature increases, oxide compound (CuO) would replace the chloride compound, which is unfavorable for the complex reaction and sulfur removal ability.

**Conclusions**

Results have demonstrated that the bentonites loaded with



**Figure 7.** DSC-TGA curves in nitrogen for the Cu(II)-bentonite adsorbent and raw bentonite.

range of 0-200 $^{\circ}$C was caused by the evaporation of water adsorbed in the bentonite and the dehydration of crystal water in $CuCl_2·2H_2O$. The peak in the range of 200-400 $^{\circ}$C was made by the $CuCl_2$ transformed into CuCl and the production of CuO. The peak above 400 $^{\circ}$C was caused by
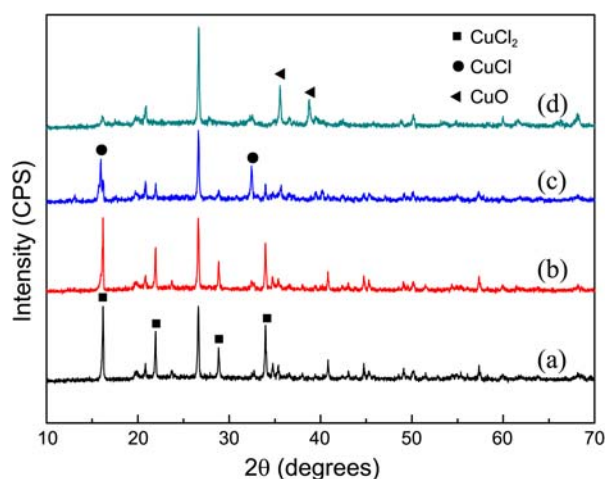
$CuCl_2$ are excellent adsorbents for the removal of DMS and PM from liquid fuels. The bentonite loaded with 15 wt % Cu(II) and baked at 150 $^o$C exhibited a sulfur adsorption capacity about 235 mg-S/g of adsorbent in the desulfurization of model oil containing about 2000 ppm DMS and 2000 ppm PM. On the basis of complex adsorption reaction and hybrid orbital theory, the adsorption of DMS on modified bentonite occurred *via* multilayer intermolecular forces and S-M ($\sigma$) bonds. The characteristic of the Cu-S and C-S stretching vibrations were found in the Raman spectrum of the Cu(II) complexe. And the FT-IR analyses indicated that the weak Lewis acid sites contributed to the adsorption of sulfur compounds.

## References

1. Subramani, V.; Song, C. S.; Mark, H. E.; Chin, Y. H. *Ind. Eng. Chem. Res*. **2005**, *44*, 5740.
2. Fakhry, S. A.; Amir, H. G.; Seyed, F. A.; Roghayeh, K. M. *Fuel Process. Technol.* **2009**, *90*, 1459.
3. Arturo, J. H.; Ralph, T. Y. *Catal. Rev.* **2004**, *46*, 111.
4. Guy, W.; Frederic, B.; Jean, P. B.; Christian, P.; Pascal, M.; Michel, T. *Microporous Mesoporous Mater.* **2008**, *109*, 184.
5. Ma, X. L.; Subramani, V.; Kim, J. H.; Song, C. S. *Appl. Catal. B* **2005**, *56*, 137.
6. Tang, X. L.; Qian, W.; Hu, A.; Zhao, Y. M.; Fei, N. N.; Shi, L. *Ind. Eng. Chem. Res.* **2011**, *50*, 9363.
7. Mykola, S.; Teresa, J. B. *Fuel Process. Technol.* **2010**, *91*, 693.
8. Yahia, A. A.; Hisham, S. B. *Fuel.* **2009**, *88*, 87.
9. Kim, D. J.; Yie, J. E. *Journal of Colloid and Interface Science* **2005**, *283*, 311.
10. Zhou, A. N.; Ma, X. L.; Song, C. S. *J. Phys. Chem. B* **2006**, *110*, 4699.
11. Arturo, J. H.; Ralph, T. Y. *AIChE J.* **2004**, *50*, 791.
12. Arturo, J. H.; Frances, H. Y.; Gongshin, Q.; Ralph, T. Y. *Appl. Catal. B* **2005**, *56*, 111.
13. Tang, X. L.; Shi, L. *Langmuir* **2011**, *27*, 11999.
14. Erson, S. E.; Nyberg, G. L. *J. Electron. Spectrosc.* **1990**, *52*, 735.
15. Doyle, A.; Tristao, M. L. B.; Felcman, J. *Fuel* **2006**, *85*, 2195.
16. Arturo, J. H.; Ralph, T. Y. *J. Am. Chem. Soc.* **2004**, *126*, 992.
17. Ryan, G. H.; Xie, X. J.; Sofia, R. P.; Isabel, M.; Edward, I. S. *Journal of Inorganic Biochemistry* **2012**, *115*, 155.
18. Noh, J.; Jang, S.; Lee, D.; Shin, S.; Young, J. K.; Eisuke, I.; Joo, S. W. *Current Applied Physics* **2007**, *7*, 605.
19. Cho, S. I.; Park, E. S.; Kim, K.; Kim, M. S. *Journal of Molecular Structure* **1999**, *479*, 83.
20. Kalita, P.; Gupta N. M.; Kumar, R. J. *Catal.* **2007**, *245*, 338.
21. Salame, I. I.; Bandosz, T. J. *Langmuir* **1999**, *15*, 587.